

Supporting Information for
Oxygen-Enriched Carbon Material for Catalyzing Oxygen
Reduction towards Hybrid Electrolyte Li-Air Battery

Shan Wang[†], Shanmu Dong[†], Jun Wang, Lixue Zhang, Pengxian Han, Chuanjian

Zhang, Xiaogang Wang, Kejun Zhang, Zhenggang Lan*, Guanglei Cui*

Qingdao Institute of Bioenergy and Bioprocess Technology, Chinese Academy of Sciences, Qingdao 266101, P. R. China.

1. Supporting results and discussion.

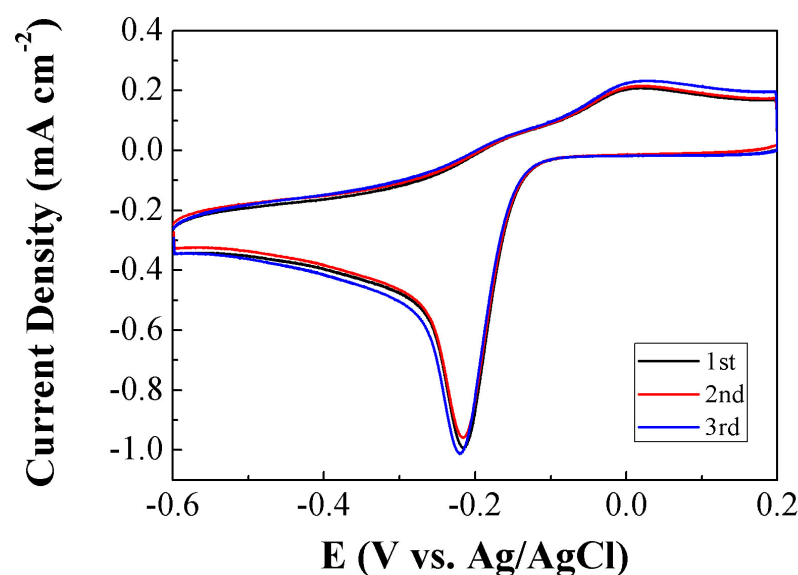


Figure S1. CV curves of GO/CNT electrode at different cycles in 1 M LiNO₃ + 0.5 M LiOH electrolyte saturated with O₂ at a scan rate of 20 mV s⁻¹.

All CV measurements were conducted in a O₂ or Ar saturated electrolyte. The CVs were scanned until we got a stabilized curve which was not changing with the cycle increasing and that curve wasd presented in the text.

1.1 Physical characterization

As shown in Fig. S2, the hybrid with a GO to CNT ratio of 1:4 exhibits a more positive onset potential and reduction peak potential of ORR, as well as a higher peak current density. Thus we used this ratio to prepare hybrid material for further investigation in this study.

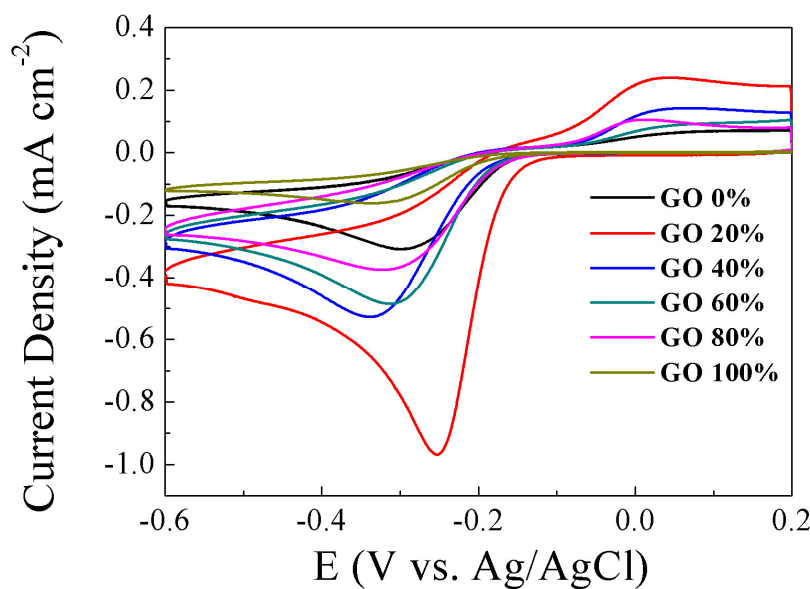


Figure S2. CV curves of GO/CNT electrodes in various proportions of GO to CNT in 1 M $\text{LiNO}_3 + 0.5 \text{ M LiOH}$ electrolyte saturated with O_2 at a scan rate of 20 mV s^{-1} .

Fig. S3 shows the C1s XPS spectra of GO, CNT, GO and CNT thermal-treated at 800 °C (denoted as GO-TR800 and CNT-TR800). The spectra of GO present clearly decreased content of oxygen-containing groups after thermal treatment, while the CNT spectra change slightly after thermal treatment.

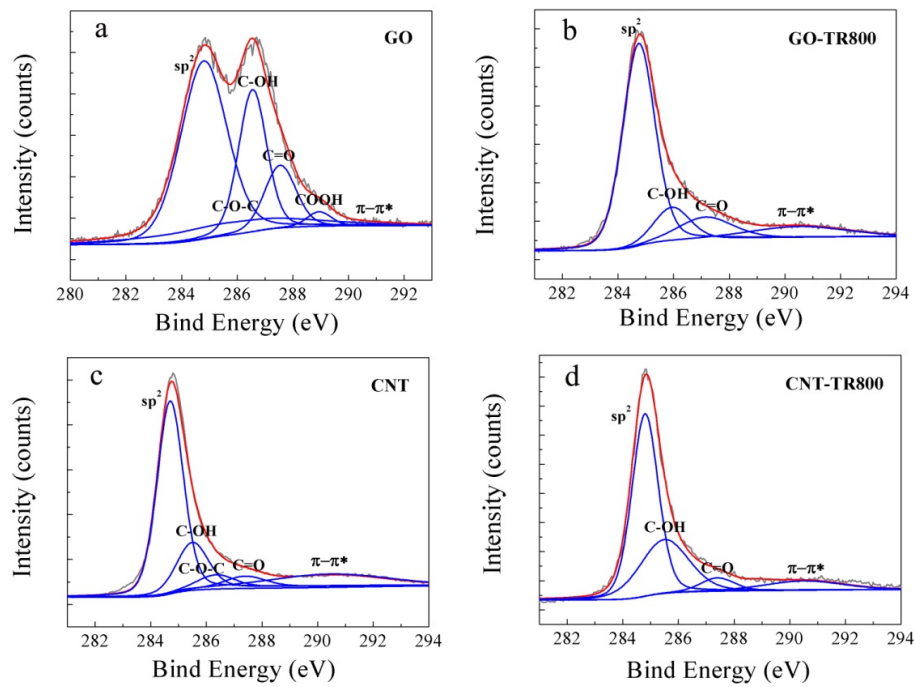


Figure S3. High-resolution C1s XPS spectra for GO (a), GO-TR800 (b), CNT (c) and CNT-TR800 (d).

Raman spectra are presented in Fig. S4. Both GO and CNT show an increased I_D/I_G ratio, indicating increased defects caused by removal of oxygen-containing groups.¹ The higher $I_{2D}/(I_D+G)$ ratio for GO after thermal treatment suggests the restoration of aromatic C-structure upon thermal treatment.²

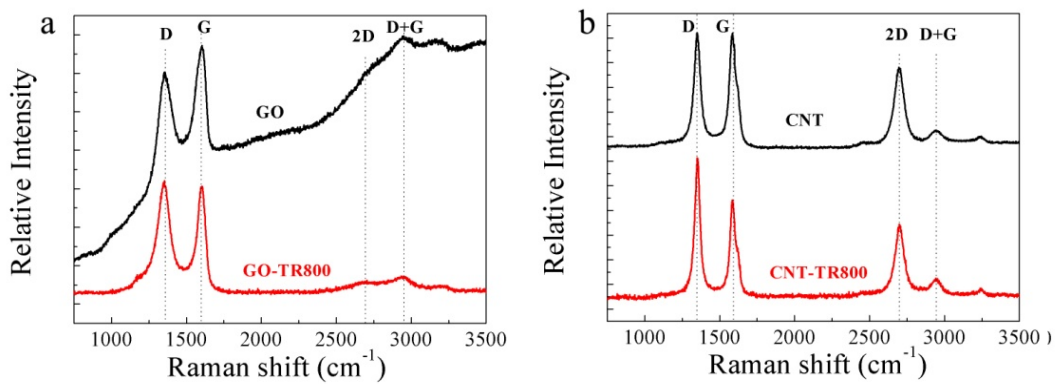


Figure S4. Raman spectra of GO, GO-TR800 (a) and CNT, CNT-TR800 (b).

1.2 Electrochemical characterization

RDE linear sweep voltammetry curves at various rotating speeds are shown in Fig. 6.

The number of electrons involved in the ORR can be calculated from the Koutecky-Levich (K-L) equation³:

$$\frac{1}{j} = \frac{1}{j_k} + \frac{1}{B\omega^{0.5}}$$

where j_k is the kinetic current and ω is the electrode rotating rate. B could be calculated from the slope of K-L plots which is determined by:

$$B = 0.2nF(D_{O_2})^{2/3}\nu^{-1/6}C_{O_2}$$

where n represents the number of electrons transferred per oxygen molecule, F is the Faraday constant ($F = 96485 \text{ C}\cdot\text{mol}^{-1}$), D is the diffusion coefficient of O_2 in 1 M $\text{LiNO}_3 + 0.5 \text{ M LiOH}$ electrolyte ($1.9 \times 10^{-5} \text{ cm}^2\cdot\text{s}^{-1}$), ν is the kinematic viscosity ($0.01 \text{ cm}^2\cdot\text{s}^{-1}$) and C_{O_2} is the bulk concentration of O_2 ($1.2 \times 10^{-6} \text{ mol}\cdot\text{cm}^{-3}$). The constant 0.2 is adopted when the rotation speed is expressed in rpm.

The conductivity measurements were conducted using the four-probe method (Table S1). The conductivity of the hybrid shows a slight increase after thermal treatment. Although the total amount of oxygen doesn't change significantly for GO/CNT-TR800, some inner transformation, such as from C-O-C to C-OH, occurs on the surface of graphene oxide during annealing⁴. This result is also confirmed by the O1s spectra (Fig. 2 e, f). According to Xu et al.⁵, the C-O-C groups show a larger influence on the conductivity of graphene oxide than hydroxyl ones. Thus a slightly higher conductivity for GO/CNT-TR800 may result from the transformation of C-O-C to C-OH.

Table S1. Conductivity measurements using the four-probe method

Sample	GO/CNT	GO/CNT -TR600	GO/CNT-TR800
Conductivity (S/cm)	8.8	9.1	11.3

Tafel slope and exchange current density are obtained from Tafel plots (Fig. S5, Table S2). The Tafel slope values of about 60 mV dec^{-1} indicate the Temkin adsorption isotherm of oxygen intermediates to the hybrids⁶. After thermal-treated at 800°C , the exchange current density for the GO/CNT hybrid decreases by one order of magnitude, confirming the lower electrocatalytic activity of the hybrid after the removal of oxygen-containing groups.

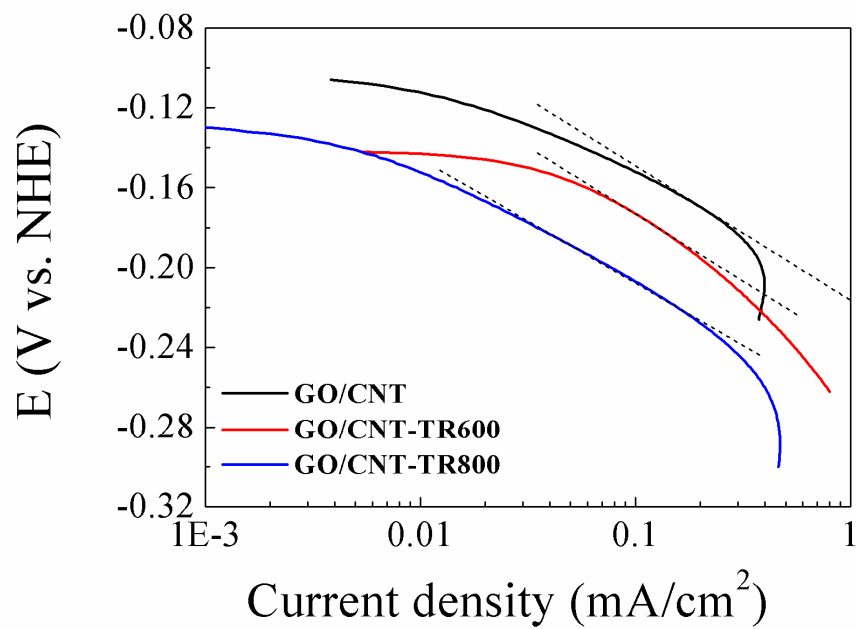


Figure S5. Tafel plots of the hybrid and thermal-treated hybrid in O_2 saturated $1\text{ M LiNO}_3 + 0.5\text{ M LiOH}$ electrolyte measured at a scan rate of 20 mV s^{-1} .

Table S2. ORR kinetic data for the hybrid obtained from Tafel plots.

Sample	GO/CNT	GO/CNT -TR600	GO/CNT-TR800
Tafel slope (mV dec ⁻¹)	66	65	61
Exchange current density (A cm ⁻²)	6.874×10^{-7}	2.894×10^{-7}	5.322×10^{-8}

Figure S6 shows the charge-discharge curves from the first cycle to the 20th cycle for Li-air batteries with GO/CNT as catalysts at a current density of 0.25 mA cm⁻², with charge and discharge for 30 minutes each. The voltage gap increases with the number of charge-discharge cycles increases, due to the limited solubility of the discharge product LiOH.

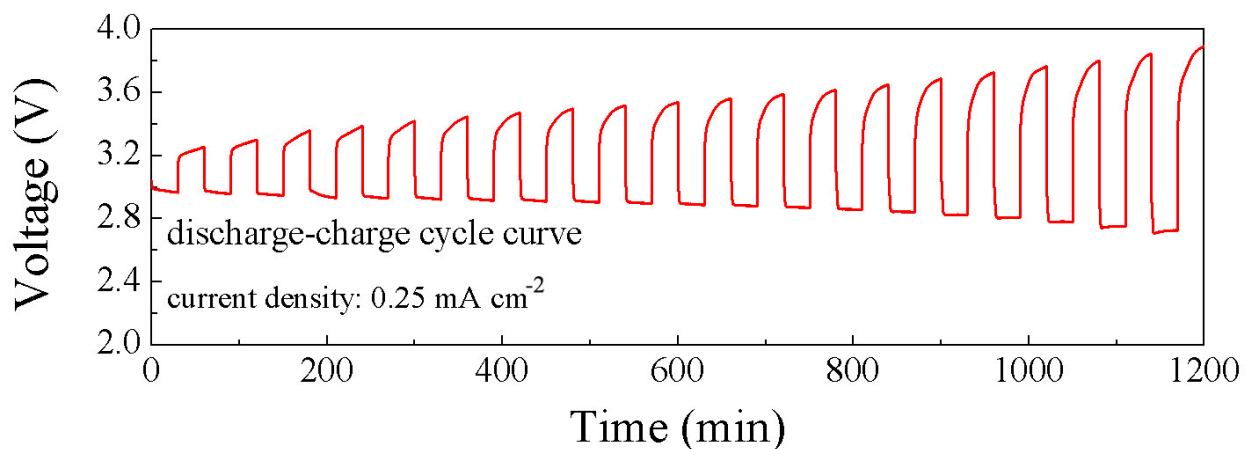


Figure S6. Charge-discharge curves of a Li-air cell using GO/CNT as cathode, lithium disks as anode, and a LISICON film as a membrane to separate the organic (1 M LiPF₆ in EC/DMC) and aqueous (1M LiNO₃ + 0.5 M LiOH) electrolytes at a current density of 0.25 mA cm⁻² from 1st to 20th cycles.

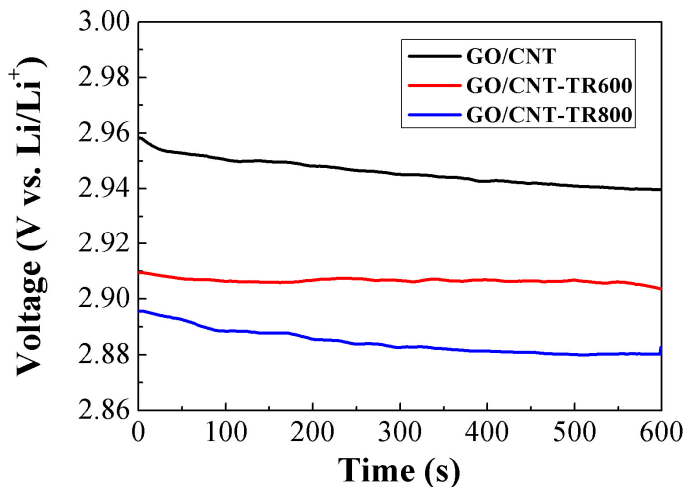


Figure S7. Comparation of discharge curves of a Li-air cell using GO/CNT, GO/CNT-TR600, GO/CNT-TR800 as cathode.

As has been shown in Figure S7, when used as cathode of Li-air cell, the thermal treated hybrids show a lower discharge plateau, which farther provide evidence for the function of oxygen-containing groups.

2. Computational details

2.1 Model construction

The model with 14 six-member rings (Figure S8) was constructed to mimic graphene. This model [donated as G(14R)] included 58 atoms and the similar model was taken in previous studies on graphene derivatives⁷. Two different types of O-decorated graphenes were introduced to represent graphene oxides. In the first type, one O atom was added to bond with two central C atoms of G(14R) (C_A and C_B in Figure S8). In the second case, one OH group was added at the C_A atom site and one additional H atom was introduced to saturate the C_B atom. Two types of graphene oxides were labeled as GO(14R)-1 and GO(14R)-2.

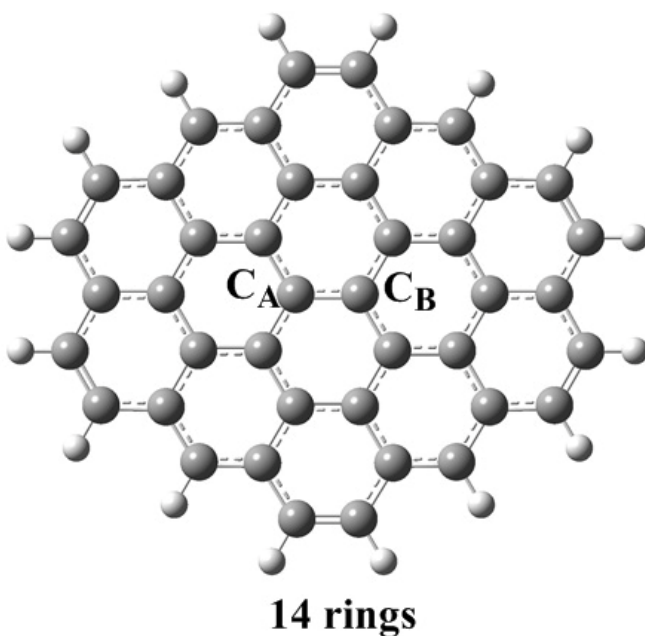


Figure S8. Molecular structures of model graphene sheet with 14 six-member rings.

Two C atoms (C_A and C_B) are in the central of the graphene sheet. Both C_C atom and C_B atom are binding with same C atom.

2.2. Absorption of O₂ on G(14R), GO(14R)-1 and GO(14R)-2.

The absorption of a single O₂ molecule on G(14R), GO(14R)-1 and GO(14R)-2 were investigated from theoretical calculations. For convenience the molecular complexes formed by absorption processes are named as adsorbate@substrate, [O₂@G(14R), O₂@GO(14R)-1 and O₂@GO(14R)-2]. All of these species were optimized at the B3LYP/6-31+G* level by Gaussian 09 software ⁸. Both singlet and triplet states were considered to describe possible spin-polarization effect. RB3LYP/6-31+G* and UB3LYP/6-31+G* were employed for close-shell and open-shell cases, respectively. The Polarizable Continuum Model (PCM) was used to include solvent (water) effect. The absorption energy (AE) is calculated by:

$AE(\text{abs}) = E(\text{ground-state complex}) - E(\text{ground-state O}_2) - E(\text{ground-state substrate})$.

All relevant geometries in their ground states are given in Figure 7-8. Their energies are given in Table S3.

Table S3. The energies (a.u.) of O_2 , substrates [G(14R), GO(14R)-1 and GO(14R)-2] and complexes [$\text{O}_2@\text{G}(14\text{R})$, $\text{O}_2@\text{GO}(14\text{R})\text{-1}$ and $\text{O}_2@\text{GO}(14\text{R})\text{-2}$] obtained at B3LYP/6-31+G* level. The absorption energies (AE) are given in the unit of kcal/mol.

	O_2	substrate	complex	AE
G14R	-150.327577	-1610.405308	-1760.723907	5.63
GO(14R)-1	-150.327577	-1685.538101	-1835.891247	-16.04
GO(14R)-2	150.327577	1686.745433	1837.073504	-0.31

We notice that the absorption of O_2 on G(14R) is not favorable since this is an endothermal reaction. As a contrast, the O_2 absorption on GO(14R)-1 becomes spontaneous, since the absorption lower the total energy of the whole system. In this sense, the inclusion of the oxygen-containing groups into graphene significantly enhances the probability of O_2 absorption.

2.3 Primary step of ORR: reactions between absorbed complexes and one water molecule

To get the first impression on the insight of ORR, the primary reaction between absorbed complexes [$\text{O}_2@\text{GO}(14\text{R})\text{-1}$] and one single H_2O molecule was examined

briefly. The reactants (absorbed O₂ and one free H₂O), the products (absorbed OOH and one free OH⁻ anion) and intermediates (absorbed OOH and absorbed OH) were optimized also at the B3LYP level. The spin polarization was also considered here. In this step, several initial guess geometries should be taken as the initial structures in optimizations and thus a large number of optimization jobs were required. For this purpose, the ORCA⁹ program was employed and the RIJCOSX¹⁰ approximation was also used to speed up DFT calculations. Thus the def2-SVP¹¹ basis set was taken for its high performance in the RIJCOSX approximation. Two or four additional electrons were added into the whole systems to mimic the 2-electron or 4-electron pathway.

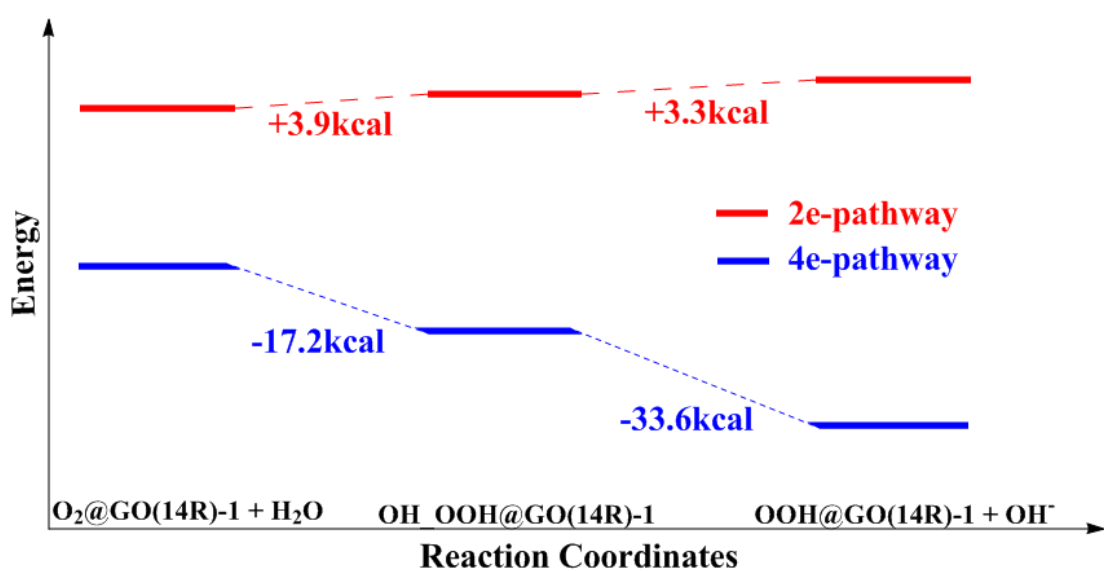


Figure S9. Energy plots of reaction between O₂@GO (14R)-1 and H₂O via the 2e-pathway (red line) and 4e-pathway (blue line). The corresponding optimized structures of reactant, product and reaction intermediate are in Figure S10.

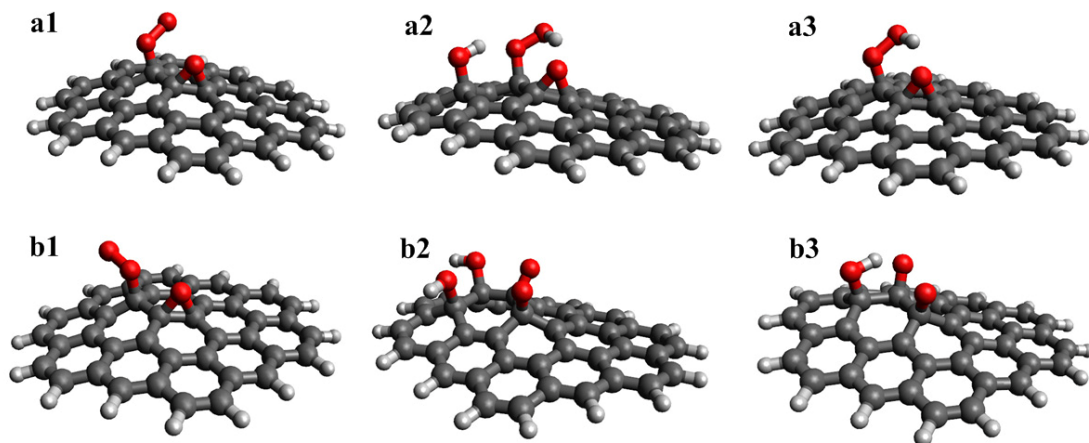


Figure S10. The optimized configurations of reactant, product and reaction intermediate for 2e-pathway (a1-3) and 4e-pathway (b1-3) at the B3LYP/DEF2-SVP level using ORCA software.

The energy from reactants to products via intermediates rises slightly with the participant of two electrons, see Figure S9. However, this reaction becomes spontaneous when four electrons are involved. Such difference can be understood by the structures of intermediates and products. With two additional electrons, the intermediate includes one absorbed OOH and one absorbed OH. With four additional electrons, the intermediate in fact contain one absorbed O and two absorbed OH. In the later case, all O atoms are connected with C atoms in the GO sheet. This indicates that the interaction between absorbed species and the GO sheet becomes stronger. In addition, the hydrogen bond is formed between one absorbed OH and the absorbed O in the product. This lowers the total energy of the product. Similar results have also been drawn in the calculations of Zheng, et. al. on nitrogen-containing graphene¹². Overall along the four-electron pathway, the energy of the whole system decreases

and thus the reaction becomes favorable.

2.4 Optimized Cartesian coordinates

Table S4. Cartesian coordinates (\AA) of geometry structure of G(14R) at the B3LYP/6-31+G* level.

58

C	-3.55682300	-2.47682800	0.00025100
C	-1.42215700	-1.23816700	0.00356000
C	-0.71152900	-2.46855500	-0.00193400
C	-1.43621900	-3.70974600	0.00040200
C	-2.83012200	-3.68885000	0.00032300
C	-0.70662600	0.00000000	-0.00442700
C	0.71152800	-2.46855500	0.00193600
C	1.42215700	-1.23816700	-0.00355900
C	0.70662600	0.00000000	0.00443100
C	3.55682300	-2.47682900	-0.00025300
C	2.83012200	-3.68885000	-0.00032400
C	1.43621900	-3.70974600	-0.00039900
C	0.68104800	-4.94063700	-0.00016500
C	-0.68104800	-4.94063700	0.00017000
H	-1.22879700	-5.88008400	0.00031900
H	1.22879700	-5.88008400	-0.00031000
H	-3.37681500	-4.62962100	0.00085800

H	3.37681400	-4.62962100	-0.00085900
C	-3.55682300	2.47682800	0.00024900
C	-2.83012200	3.68885000	0.00032200
C	-1.43621900	3.70974600	0.00040200
C	-0.71152900	2.46855500	-0.00193200
C	-1.42215700	1.23816700	0.00356000
C	-2.84478700	1.23739000	-0.00197500
C	-0.68104800	4.94063700	0.00017000
C	0.71152900	2.46855500	0.00193400
C	1.43621900	3.70974600	-0.00039900
C	0.68104800	4.94063700	-0.00016500
C	2.83012200	3.68885000	-0.00032200
H	3.37681400	4.62962100	-0.00085500
C	3.55682300	2.47682900	-0.00025100
C	2.84478700	1.23739000	0.00197000
C	1.42215700	1.23816700	-0.00355900
H	-1.22879700	5.88008400	0.00031900
H	-3.37681400	4.62962100	0.00085500
H	1.22879700	5.88008400	-0.00031000
C	-2.84478700	-1.23739000	-0.00197600
C	-3.55961300	0.00000000	0.00171200
C	2.84478700	-1.23739000	0.00197100

C	3.55961300	0.00000000	-0.00170800	
C	-4.98636100	-2.44212800	-0.00004000	
C	-5.66959000	-1.25051900	-0.00024800	
H	-6.75710900	-1.24667600	-0.00044000	
C	-4.98137600	0.00000000	-0.00024100	
C	-5.66959000	1.25051900	-0.00025000	
C	-4.98636100	2.44212800	-0.00004300	
C	4.98636100	-2.44212800	0.00003600	
C	5.66959000	-1.25051900	0.00024600	
H	6.75710900	-1.24667600	0.00043800	
C	4.98137600	0.00000000	0.00023800	
C	4.98636100	2.44212800	0.00003900	
C	5.66959000	1.25051900	0.00024800	
H	5.53071000	-3.38343700	-0.00011800	
H	6.75710900	1.24667600	0.00044000	
H	5.53071000	3.38343700	-0.00011200	
H	-5.53071000	3.38343700	0.00010700	
H	-6.75710900	1.24667600	-0.00044300	
<hr/>	H	-5.53071000	-3.38343700	0.00011200

Table S5. Cartesian coordinates (\AA) of geometry structure of GO(14R)-1 at the

B3LYP/6-31+G* level.

59

C	3.56165800	-2.48511500	-0.10690200
C	1.45197400	-1.26771700	0.16904800
C	0.72624900	-2.46819600	0.11125100
C	1.43632800	-3.70618800	-0.03130100
C	2.83269900	-3.68906500	-0.11308700
C	0.75012400	0.00000900	0.44690500
C	-0.72623800	-2.46819300	0.11119900
C	-1.45197400	-1.26771600	0.16892300
C	-0.75013500	0.00001500	0.44675600
C	-3.56166100	-2.48512300	-0.10690000
C	-2.83269400	-3.68907200	-0.11308400
C	-1.43632400	-3.70619200	-0.03130700
C	-0.68054600	-4.93553300	-0.10410300
C	0.68054700	-4.93552800	-0.10411500
H	1.22865700	-5.87145800	-0.18064500
H	-1.22865200	-5.87146700	-0.18061500
H	3.36982600	-4.63068500	-0.20614300
H	-3.36981700	-4.63069800	-0.20612100
C	3.56166000	2.48511700	-0.10688800
C	2.83269500	3.68906400	-0.11307800

C	1.43632600	3.70618900	-0.03128800
C	0.72624800	2.46819500	0.11127700
C	1.45198200	1.26771400	0.16907800
C	2.85259700	1.24779300	0.02108900
C	0.68054900	4.93552900	-0.10412000
C	-0.72623700	2.46819400	0.11122400
C	-1.43631900	3.70619400	-0.03130800
C	-0.68054400	4.93553500	-0.10411600
C	-2.83268800	3.68907300	-0.11310000
H	-3.36981000	4.63069800	-0.20615100
C	-3.56166200	2.48512800	-0.10691100
C	-2.85259700	1.24780200	0.02100300
C	-1.45198500	1.26771800	0.16894600
H	1.22866300	5.87145600	-0.18066100
H	3.36982500	4.63068400	-0.20613000
H	-1.22865200	5.87146700	-0.18064800
C	2.85258900	-1.24779400	0.02107500
C	3.56758100	-0.00000100	-0.02082800
C	-2.85258700	-1.24780000	0.02099900
C	-3.56757000	0.00000100	-0.02090200
C	4.99015600	-2.44514400	-0.22572400
C	5.66381100	-1.25281100	-0.24694200

H	6.74661600	-1.24035400	-0.34563300
C	4.97036800	0.00000100	-0.16307500
C	5.66381000	1.25281200	-0.24693100
C	4.99015700	2.44514700	-0.22571200
C	-4.99016300	-2.44515200	-0.22566400
C	-5.66381200	-1.25281400	-0.24688700
H	-6.74662100	-1.24035400	-0.34553100
C	-4.97036200	0.00000100	-0.16307400
C	-4.99016200	2.44515600	-0.22568200
C	-5.66380800	1.25281500	-0.24689400
H	-5.53310800	-3.38348900	-0.30833500
H	-6.74661800	1.24035300	-0.34553500
<u>H</u>	-5.53311100	3.38349000	-0.30836500
H	5.53309800	3.38348200	-0.30843600
H	6.74661600	1.24035300	-0.34561300
H	5.53309500	-3.38348000	-0.30845200
O	<u>-0.00003000</u>	<u>-0.00003700</u>	<u>1.70623800</u>

Table S6. Cartesian coordinates (\AA) of geometry structure of GO(14R)-2 at the B3LYP/6-31+G* level.

C	-3.58746800	2.47618600	-0.12392500
C	-1.47358500	1.26477200	0.22039700
C	-0.75992100	2.45607000	0.07734700
C	-1.46721500	3.68776900	-0.14139500
C	-2.86116000	3.67737300	-0.20387300
C	-0.80392100	0.00001100	0.70713000
C	0.69392800	2.45065800	0.07730800
C	1.41274500	1.25885000	0.22889000
C	0.75157900	-0.00001000	0.75849100
C	3.52034900	2.47125500	-0.16604500
C	2.79228200	3.67053900	-0.23482400
C	1.39869200	3.68101900	-0.15522000
C	0.64650000	4.90464600	-0.30711700
C	-0.71290300	4.90857400	-0.29911700
H	-1.26162900	5.83774000	-0.43310200
H	1.19877000	5.83068300	-0.44793500
H	-3.39648300	4.61426500	-0.34288700
H	3.32466500	4.60759100	-0.38414300
C	-3.58750600	-2.47615400	-0.12381700
C	-2.86121100	-3.67735000	-0.20375800
C	-1.46726400	-3.68775400	-0.14133300
C	-0.75994900	-2.45605800	0.07737200

C	-1.47360200	-1.26475400	0.22044400
C	-2.87698500	-1.24697300	0.06683300
C	-0.71296900	-4.90856600	-0.29908400
C	0.69390200	-2.45066100	0.07727500
C	1.39864400	-3.68102800	-0.15528500
C	0.64643300	-4.90464800	-0.30714900
C	2.79223100	-3.67056000	-0.23494600
H	3.32460100	-4.60761200	-0.38430600
C	3.52030900	-2.47128300	-0.16616200
C	2.81331000	-1.24296000	0.04027600
C	1.41273100	-1.25885700	0.22884100
H	-1.26171000	-5.83772700	-0.43304200
H	-3.39654400	-4.61424200	-0.34273000
H	1.19868900	-5.83068900	-0.44799800
C	-2.87696500	1.24700000	0.06677400
C	-3.59668300	0.00001900	0.05537700
C	2.81333200	1.24293300	0.04034600
C	3.53535600	-0.00002000	0.00771400
C	-5.01680500	2.43840300	-0.22607300
C	-5.69427000	1.24971500	-0.19921100
H	-6.77784800	1.23560500	-0.29001800
C	-4.99999200	0.00002700	-0.09524700

C	-5.69429100	-1.24965600	-0.19913400
C	-5.01684400	-2.43835500	-0.22594300
C	4.94674700	2.43659400	-0.30297700
C	5.62702700	1.24925000	-0.29506900
H	6.70780600	1.23589200	-0.41333200
C	4.93486400	-0.00002400	-0.17573400
C	4.94670600	-2.43663500	-0.30311600
C	5.62700700	-1.24930300	-0.29515200
H	5.48009400	3.37582700	-0.42791100
H	6.70778500	-1.23595300	-0.41342800
H	5.48003500	-3.37587100	-0.42810600
H	-5.55565400	-3.37629600	-0.33668800
H	-6.77787000	-1.23553400	-0.28992700
H	-5.55559800	3.37634700	-0.33687400
O	0.99042100	-0.00007000	2.22131000
H	1.95145200	0.00015000	2.37749300
<u>H</u>	<u>-1.05291500</u>	<u>0.00004400</u>	<u>1.78378800</u>

Table S7. Cartesian coordinates (\AA) of geometry structure of $\text{O}_2@\text{G}(14\text{R})$ at the B3LYP/6-31+G* level.

C	-3.56899500	2.47644400	-0.19709300
C	-1.43164000	1.24407200	-0.21006600
C	-0.72421900	2.47587800	-0.19961200
C	-1.45202200	3.71455200	-0.19432500
C	-2.84497400	3.68896000	-0.19183900
C	-0.71283200	0.00819300	-0.21149900
C	0.69830400	2.47974100	-0.20752900
C	1.41226200	1.25168600	-0.20823000
C	0.70018800	0.01198800	-0.22102300
C	3.54299200	2.49549600	-0.21013500
C	2.81251200	3.70414200	-0.20278800
C	1.41942900	3.72233100	-0.19967100
C	0.66099900	4.94999900	-0.19205600
C	-0.70022600	4.94630200	-0.18940300
H	-1.25079200	5.88445900	-0.18352300
H	1.20647300	5.89113500	-0.18826600
H	-3.39424100	4.62875600	-0.18647400
H	3.35678600	4.64684600	-0.19846700
C	-3.55577000	-2.47530400	-0.22153900
C	-2.82525300	-3.68392700	-0.22749300
C	-1.43216200	-3.70207400	-0.22938800
C	-0.71101700	-2.45950400	-0.22289400

C	-1.42505800	-1.23148000	-0.22178800
C	-2.84734300	-1.23440600	-0.21465700
C	-0.67377500	-4.92978000	-0.23528900
C	0.71152500	-2.45571100	-0.22889700
C	1.43928600	-3.69440900	-0.23304800
C	0.68745200	-4.92613900	-0.23694700
C	2.83223400	-3.66879800	-0.23490800
H	3.38153600	-4.60858400	-0.23919000
C	3.55619400	-2.45623800	-0.23144400
C	2.84110800	-1.21916600	-0.22657900
C	1.41888000	-1.22390300	-0.22251700
H	-1.21928900	-5.87089500	-0.23860100
H	-3.36950000	-4.62664700	-0.23151800
H	1.23797800	-5.86432900	-0.24148200
C	-2.85392200	1.23937800	-0.20252800
C	-3.56530100	0.00060400	-0.21136800
C	2.83450800	1.25463500	-0.21709700
C	3.55246300	0.01964000	-0.22071800
C	-4.99741800	2.43742600	-0.19493700
C	-5.67715300	1.24485700	-0.20005200
H	-6.76499900	1.23810900	-0.19834000
C	-4.98660600	-0.00321000	-0.20747100

C	-5.67046600	-1.25497500	-0.21259900
C	-4.98439400	-2.44390300	-0.21931300
C	4.97161300	2.46410400	-0.21310500
C	5.65766300	1.27516400	-0.21960800
H	6.74553200	1.27422200	-0.22135400
C	4.97377000	0.02341100	-0.22381300
C	4.98461500	-2.41723500	-0.23331400
C	5.66433600	-1.22465700	-0.22981500
H	5.51337000	3.40728800	-0.20960300
H	6.75218500	-1.21788700	-0.23136000
H	5.53136900	-3.35752500	-0.23777000
H	-5.52614900	-3.38708500	-0.22314400
H	-6.75833400	-1.25405900	-0.21094300
H	-5.54416100	3.37771300	-0.18924200
O	0.61656300	-0.43564900	3.40349400
O	<u>-0.40262300</u>	<u>0.09732200</u>	<u>3.79646200</u>

Table S8. Cartesian coordinates (Å) of geometry structure of O₂@GO(14R)-1 at the B3LYP/6-31+G* level.

61

C	-3.78807900	2.45165000	0.04579200
C	-1.59295900	1.36527500	0.14411000

C	-0.95456100	2.61338600	0.22095900
C	-1.75253300	3.80500800	0.23882900
C	-3.14570200	3.69725300	0.17460700
C	-0.79807400	0.12732300	0.25586800
C	0.49377700	2.71809500	0.19966700
C	1.30291400	1.57495300	0.10100600
C	0.69846600	0.23567500	0.23349400
C	3.31471700	2.96608800	-0.06044900
C	2.50367200	4.10623400	0.09139200
C	1.11201900	4.01231700	0.19685300
C	0.27071200	5.18367500	0.28525400
C	-1.08645900	5.08553900	0.30489800
H	-1.69967400	5.98122600	0.35108600
H	0.74971300	6.15832400	0.31577300
H	-3.74887700	4.60126000	0.20360400
H	2.97070000	5.08784400	0.10553900
C	-3.44086900	-2.46973600	-0.55454300
C	-2.63006000	-3.60833100	-0.71858800
C	-1.23446100	-3.53407900	-0.66046100
C	-0.60955800	-2.27444300	-0.37816400
C	-1.41578500	-1.14526000	-0.16327600
C	-2.81731100	-1.20886200	-0.28754400

C	-0.39673600	-4.68770900	-0.89503600
C	0.83874300	-2.16932100	-0.40066200
C	1.62977100	-3.32651300	-0.70409400
C	0.96041400	-4.58928700	-0.91587000
C	3.01911200	-3.19916100	-0.80439400
H	3.61757800	-4.08109500	-1.01871700
C	3.66200900	-1.95529900	-0.66247200
C	2.87168900	-0.79685000	-0.37359800
C	1.48006900	-0.93551200	-0.20693000
H	-0.87936100	-5.64386000	-1.07727400
H	-3.10161600	-4.56758800	-0.91699000
H	1.57003100	-5.46637200	-1.11465100
C	-2.99163300	1.26229000	0.01395500
C	-3.61836000	-0.01980900	-0.16802300
C	2.69728000	1.67424000	-0.07136100
C	3.49642700	0.49549600	-0.27602100
C	-5.21250600	2.32329700	-0.05729200
C	-5.80137600	1.09678600	-0.21289100
H	-6.88174800	1.01834300	-0.29749200
C	-5.02045900	-0.10388600	-0.28975500
C	-5.62638900	-1.38444100	-0.51396500
C	-4.87102900	-2.51896700	-0.64659700

C	4.73899900	3.04404400	-0.20713500
C	5.49331200	1.91489800	-0.38441500
H	6.57058600	1.99285800	-0.50223200
C	4.89153400	0.61407000	-0.44073700
C	5.08081600	-1.79813600	-0.79800500
C	5.66859700	-0.56631400	-0.68636900
H	5.21248300	4.02158400	-0.18439500
H	6.74430500	-0.46406200	-0.79998100
H	5.68552100	-2.67740000	-1.00166300
H	-5.34859200	-3.47671800	-0.83371500
H	-6.70856000	-1.43832600	-0.59439500
H	-5.82073500	3.22259900	-0.01868500
O	-0.02019700	0.03023300	1.49413200
O	0.95114700	-3.53323000	3.18892800
O	1.13746900	-4.58733800	3.76393600

Table S9. Cartesian coordinates (Å) of geometry structure of O₂@GO(14R)-2 at the B3LYP/6-31+G* level.

63

C	-3.73430500	2.55580500	0.02058400
C	-1.56309100	1.41209600	0.19953300
C	-0.90618700	2.64394400	0.19530500

C	-1.67162500	3.85856500	0.13177100
C	-3.06439400	3.79060400	0.07931100
C	-0.83022200	0.13100300	0.52612300
C	0.54628900	2.70615100	0.18470200
C	1.32070400	1.53972300	0.18743900
C	0.72394100	0.19686500	0.56529700
C	3.36559300	2.88792000	-0.07439000
C	2.58282400	4.05142400	0.00671500
C	1.19130700	3.98712200	0.09677200
C	0.38236200	5.18364500	0.09842900
C	-0.97561300	5.12336400	0.11664200
H	-1.56740700	6.03547900	0.09965600
H	0.89032100	6.14449600	0.06590100
H	-3.64371800	4.71126600	0.05818300
H	3.07011800	5.02340900	-0.03288300
C	-3.50972000	-2.35609500	-0.57066800
C	-2.73057100	-3.50341300	-0.80195000
C	-1.33678600	-3.45543700	-0.75490300
C	-0.68318600	-2.22715600	-0.39516900
C	-1.44837300	-1.09664600	-0.10277400
C	-2.85314300	-1.12641700	-0.24072400
C	-0.53005900	-4.61111200	-1.06770700

C	0.76869000	-2.15312700	-0.40824800
C	1.52528600	-3.31248100	-0.79297700
C	0.82752000	-4.54219000	-1.08762600
C	2.91583300	-3.22784000	-0.88066500
H	3.48794300	-4.11451400	-1.14580900
C	3.58985700	-2.01341600	-0.67114100
C	2.83078200	-0.85299900	-0.31286300
C	1.43475700	-0.95655300	-0.11791200
H	-1.03778900	-5.54178800	-1.30948800
H	-3.22465700	-4.44110000	-1.04746200
H	1.41948000	-5.41715900	-1.34549800
C	-2.96618800	1.34722800	0.05683600
C	-3.62861700	0.07810100	-0.09657700
C	2.71802900	1.61199300	-0.01211500
C	3.49526600	0.41693900	-0.19922400
C	-5.16171700	2.46361200	-0.07329800
C	-5.78411400	1.24974700	-0.18220600
H	-6.86710700	1.19579200	-0.26487900
C	-5.03252000	0.03032500	-0.23338200
C	-5.67084100	-1.22938300	-0.47861400
C	-4.94069800	-2.37351600	-0.65347700
C	4.79014700	2.93642300	-0.22554100

C	5.52370400	1.78972700	-0.36587600
H	6.60223300	1.84114200	-0.49374600
C	4.89073200	0.50413900	-0.39203100
C	5.01138300	-1.89637500	-0.81217600
C	5.63727700	-0.68825900	-0.66584300
H	5.27871200	3.90769800	-0.24085900
H	6.71482800	-0.61062000	-0.78891600
H	5.58526700	-2.78804300	-1.05252400
H	-5.43798700	-3.31608900	-0.86940000
H	-6.75519700	-1.25517000	-0.55653400
H	-5.74404600	3.38181200	-0.06669400
O	0.98101600	0.03033000	2.01560500
O	0.58846900	-3.81156100	2.97613100
O	0.68655500	-4.97422100	3.31553200
H	-1.06436600	-0.00710400	1.59717600
<u>H</u>	<u>1.94317400</u>	<u>0.04982300</u>	<u>2.16332200</u>

Table S10. Cartesian coordinates (\AA) of geometry structure of reactant for the reaction of $\text{O}_2@\text{GO(14R)-1}$ and H_2O via a 2e-pathway at the B3LYP/def2-SVP level.

64

C	-3.771002	2.391951	-0.152080
C	-1.596892	1.274372	0.130553

C	-0.941104	2.520863	0.153528
C	-1.720128	3.724357	0.036741
C	-3.111421	3.634866	-0.090632
C	-0.831091	0.048418	0.446411
C	0.506353	2.596344	0.191694
C	1.305785	1.428870	0.245906
C	0.673007	0.123367	0.594084
C	3.308312	2.773723	-0.240620
C	2.526487	3.939174	-0.127297
C	1.140131	3.876675	0.043624
C	0.322016	5.068362	0.020882
C	-1.037866	4.997842	0.023734
H	-1.640399	5.909831	-0.020477
H	0.825266	6.038404	-0.030862
H	-3.699836	4.554266	-0.167508
H	3.007629	4.915861	-0.236492
C	-3.496377	-2.563479	-0.330237
C	-2.697000	-3.721531	-0.401805
C	-1.305799	-3.674044	-0.278682
C	-0.633657	-2.415315	0.005054
C	-1.455789	-1.250884	0.121047
C	-2.844523	-1.300020	-0.094899

C	-0.501093	-4.854483	-0.443672
C	0.776312	-2.371940	0.094063
C	1.551543	-3.530454	-0.203643
C	0.861908	-4.778888	-0.423053
C	2.948851	-3.445497	-0.365331
H	3.520833	-4.348216	-0.602705
C	3.588454	-2.183279	-0.421851
C	2.848573	-0.993291	-0.130527
C	1.531063	-1.159752	0.598173
H	-1.003980	-5.809560	-0.626417
H	-3.177827	-4.686410	-0.594369
H	1.461817	-5.678431	-0.599677
C	-2.995892	1.187457	-0.049474
C	-3.640641	-0.093772	-0.137952
C	2.681005	1.493660	-0.060156
C	3.447838	0.273273	-0.264151
C	-5.191432	2.280433	-0.316823
C	-5.796923	1.052859	-0.404548
H	-6.879604	0.984271	-0.549337
C	-5.040907	-0.164574	-0.334397
C	-5.666379	-1.444270	-0.495568
C	-4.915255	-2.594995	-0.506307

C	4.706480	2.833745	-0.560161
C	5.423621	1.681728	-0.767048
H	6.481639	1.739523	-1.042802
C	4.825052	0.388958	-0.651940
C	4.958152	-2.040815	-0.812194
C	5.557453	-0.803571	-0.910598
H	5.179487	3.813992	-0.665544
H	6.608424	-0.721648	-1.205782
H	5.534179	-2.944704	-1.036765
H	-5.397126	-3.564710	-0.665331
H	-6.749758	-1.487884	-0.641543
H	-5.785091	3.196515	-0.386234
O	-0.184095	0.177961	1.739854
O	1.110802	-2.187014	2.753595
O	<u>2.004419</u>	<u>-1.376952</u>	<u>1.953930</u>

Table S11. Cartesian coordinates (Å) of geometry structure of reaction intermediate for the reaction of O₂@GO(14R)-1 and H₂O via a 2e-pathway at the B3LYP/def2-SVP level.

64

C	-3.867434	2.341677	-0.088944
C	-1.637405	1.213399	0.083955

C	-1.006108	2.517037	0.058614
C	-1.811037	3.689388	-0.028631
C	-3.221243	3.592933	-0.070636
C	-0.855846	0.037471	0.201335
C	0.425308	2.614480	0.040343
C	1.236478	1.446551	0.152303
C	0.571866	0.202453	0.769199
C	3.249094	2.832486	-0.231490
C	2.449448	3.985339	-0.206698
C	1.049466	3.900070	-0.104519
C	0.213905	5.069666	-0.148746
C	-1.149327	4.969373	-0.102735
H	-1.768737	5.872053	-0.147579
H	0.693454	6.051433	-0.230226
H	-3.819675	4.508782	-0.124775
H	2.919436	4.968624	-0.320628
C	-3.534711	-2.622653	-0.255390
C	-2.734731	-3.756874	-0.366234
C	-1.314585	-3.679282	-0.318870
C	-0.655512	-2.427379	-0.057579
C	-1.474988	-1.224255	0.048424
C	-2.898482	-1.326009	-0.093935

C	-0.499827	-4.827911	-0.553995
C	0.756446	-2.345152	0.003847
C	1.547884	-3.481060	-0.365985
C	0.870338	-4.722430	-0.605251
C	2.943471	-3.359529	-0.578138
H	3.523990	-4.242833	-0.871855
C	3.583329	-2.121386	-0.433870
C	2.834165	-0.947378	-0.046748
C	1.471618	-1.145195	0.619104
H	-0.988424	-5.792602	-0.735825
H	-3.203934	-4.733974	-0.530468
H	1.474737	-5.606337	-0.845441
C	-3.066161	1.136480	-0.035745
C	-3.703394	-0.144113	-0.095123
C	2.624520	1.542507	-0.055200
C	3.425006	0.322202	-0.179664
C	-5.292088	2.206285	-0.167218
C	-5.895400	0.961787	-0.215340
H	-6.987509	0.887830	-0.287208
C	-5.138972	-0.234015	-0.192375
C	-5.737859	-1.532835	-0.289497
C	-4.976524	-2.671371	-0.325622

C	4.670212	2.909754	-0.470054
C	5.406064	1.762141	-0.623510
H	6.477309	1.825708	-0.850808
C	4.817721	0.462996	-0.523732
C	4.978381	-1.955600	-0.749982
C	5.575699	-0.718609	-0.770863
H	5.134416	3.896135	-0.570441
H	6.640396	-0.619767	-1.014899
H	5.564782	-2.849786	-0.995220
H	-5.454707	-3.652240	-0.424643
H	-6.830504	-1.601169	-0.354404
H	-5.901835	3.115499	-0.200396
O	0.424372	0.594464	2.061239
O	1.708348	-1.477182	2.014690
O	<u>2.528623</u>	<u>-2.645181</u>	<u>2.232032</u>

Table S12. Cartesian coordinates (\AA) of geometry structure of product for the reaction of $\text{O}_2@\text{GO(14R)-1}$ and H_2O via a 2e-pathway at the B3LYP/def2-SVP level.

62

C	-0.025126	0.064335	0.012633
C	-0.016584	0.004951	2.469532
C	1.390048	-0.011017	2.482936

C	2.101437	0.020781	1.234524
C	1.382119	0.082841	0.034897
C	-0.752842	0.151484	3.743655
C	2.121480	-0.152595	3.728224
C	1.455606	-0.228189	4.972052
C	0.009892	0.121819	5.040581
C	3.558015	-0.869993	6.072780
C	4.233501	-0.650495	4.857927
C	3.545989	-0.330117	3.683383
C	4.229454	-0.218356	2.414835
C	3.544596	-0.042317	1.251391
H	4.076678	0.020023	0.298048
H	5.320031	-0.306763	2.406506
H	1.927680	0.124849	-0.912412
H	5.318882	-0.787025	4.820278
C	-4.299846	-0.404915	2.484431
C	-4.961490	-0.645698	3.706755
C	-4.280275	-0.694794	4.924251
C	-2.852608	-0.431744	4.973319
C	-2.194229	-0.154723	3.740264
C	-2.879750	-0.188302	2.509546
C	-4.959821	-1.010327	6.154081

C	-2.166384	-0.503961	6.212320
C	-2.846028	-0.919873	7.397648
C	-4.274214	-1.127148	7.327126
C	-2.135808	-1.189670	8.580060
H	-2.675852	-1.510697	9.475438
C	-0.719757	-1.230621	8.572288
C	0.004569	-0.823814	7.411391
C	-0.747823	-0.045066	6.369206
H	-6.039680	-1.185412	6.121572
H	-6.041108	-0.828683	3.696556
H	-4.800829	-1.406700	8.245241
C	-0.738706	0.007980	1.255974
C	-2.173803	-0.057422	1.259090
C	2.138064	-0.660678	6.127119
C	1.407117	-0.968844	7.343377
C	-0.777781	0.096213	-1.208446
C	-2.147008	0.036317	-1.195160
H	-2.705028	0.048388	-2.135987
C	-2.881803	-0.064610	0.033639
C	-4.306749	-0.209833	0.046280
C	-4.983872	-0.390069	1.228181
C	4.247643	-1.322341	7.247133

C	3.552839	-1.618361	8.391603
H	4.082556	-1.987106	9.275579
C	2.130805	-1.477263	8.466484
C	0.032412	-1.724448	9.687467
C	1.402700	-1.831131	9.640058
H	5.332584	-1.452359	7.202123
H	1.954183	-2.208825	10.506860
H	-0.507764	-2.026918	10.590237
H	-6.068195	-0.538862	1.223182
H	-4.844447	-0.204646	-0.905794
H	-0.236416	0.158289	-2.156771
O	-0.322552	1.391258	4.424698
O	-1.706859	2.227546	6.505954
O	-0.715334	1.321116	7.040299
H	<u>-1.388949</u>	<u>2.293977</u>	<u>5.581003</u>

Table S13. Cartesian coordinates (\AA) of geometry structure of reactant for the reaction of $\text{O}_2@\text{GO(14R)-1}$ and H_2O via a 4e-pathway at the B3LYP/def2-SVP level.

64

C	-3.867434	2.341677	-0.088944
C	-1.637405	1.213399	0.083955
C	-1.006108	2.517037	0.058614

C	-1.811037	3.689388	-0.028631
C	-3.221243	3.592933	-0.070636
C	-0.855846	0.037471	0.201335
C	0.425308	2.614480	0.040343
C	1.236478	1.446551	0.152303
C	0.571866	0.202453	0.769199
C	3.249094	2.832486	-0.231490
C	2.449448	3.985339	-0.206698
C	1.049466	3.900070	-0.104519
C	0.213905	5.069666	-0.148746
C	-1.149327	4.969373	-0.102735
H	-1.768737	5.872053	-0.147579
H	0.693454	6.051433	-0.230226
H	-3.819675	4.508782	-0.124775
H	2.919436	4.968624	-0.320628
C	-3.534711	-2.622653	-0.255390
C	-2.734731	-3.756874	-0.366234
C	-1.314585	-3.679282	-0.318870
C	-0.655512	-2.427379	-0.057579
C	-1.474988	-1.224255	0.048424
C	-2.898482	-1.326009	-0.093935
C	-0.499827	-4.827911	-0.553995

C	0.756446	-2.345152	0.003847
C	1.547884	-3.481060	-0.365985
C	0.870338	-4.722430	-0.605251
C	2.943471	-3.359529	-0.578138
H	3.523990	-4.242833	-0.871855
C	3.583329	-2.121386	-0.433870
C	2.834165	-0.947378	-0.046748
C	1.471618	-1.145195	0.619104
H	-0.988424	-5.792602	-0.735825
H	-3.203934	-4.733974	-0.530468
H	1.474737	-5.606337	-0.845441
C	-3.066161	1.136480	-0.035745
C	-3.703394	-0.144113	-0.095123
C	2.624520	1.542507	-0.055200
C	3.425006	0.322202	-0.179664
C	-5.292088	2.206285	-0.167218
C	-5.895400	0.961787	-0.215340
H	-6.987509	0.887830	-0.287208
C	-5.138972	-0.234015	-0.192375
C	-5.737859	-1.532835	-0.289497
C	-4.976524	-2.671371	-0.325622
C	4.670212	2.909754	-0.470054

C	5.406064	1.762141	-0.623510
H	6.477309	1.825708	-0.850808
C	4.817721	0.462996	-0.523732
C	4.978381	-1.955600	-0.749982
C	5.575699	-0.718609	-0.770863
H	5.134416	3.896135	-0.570441
H	6.640396	-0.619767	-1.014899
H	5.564782	-2.849786	-0.995220
H	-5.454707	-3.652240	-0.424643
H	-6.830504	-1.601169	-0.354404
H	-5.901835	3.115499	-0.200396
O	0.424372	0.594464	2.061239
O	1.708348	-1.477182	2.014690
O	<u>2.528623</u>	<u>-2.645181</u>	<u>2.232032</u>

Table S14. Cartesian coordinates (Å) of geometry structure of reaction intermediate for the reaction of O₂@GO(14R)-1 and H₂O via a 4e-pathway at the B3LYP/def2-SVP level.

64

C	-0.012891	0.069744	0.015430
C	-0.029441	-0.028480	2.515197
C	1.414521	-0.001279	2.511015

C	2.104570	0.073521	1.266403
C	1.385303	0.170119	0.045388
C	-0.723424	-0.097609	3.746870
C	2.129481	-0.143471	3.749661
C	1.447841	-0.113314	5.022875
C	0.012106	0.438931	5.010301
C	3.638352	-0.352806	6.162995
C	4.278050	-0.367544	4.914346
C	3.557933	-0.248371	3.712878
C	4.232472	-0.175434	2.444608
C	3.541448	-0.000629	1.276900
H	4.075020	0.063752	0.322062
H	5.326468	-0.249026	2.431703
H	1.940174	0.266442	-0.894342
H	5.371311	-0.454187	4.873554
C	-4.166139	-1.083005	2.478915
C	-4.739626	-1.538410	3.668260
C	-4.005843	-1.555218	4.894220
C	-2.696013	-0.977754	4.946926
C	-2.065191	-0.531306	3.724887
C	-2.785790	-0.639121	2.484359
C	-4.526614	-2.164312	6.074081

C	-1.970052	-0.897220	6.171484
C	-2.459474	-1.634727	7.277521
C	-3.741547	-2.240098	7.213556
C	-1.628898	-1.762793	8.446328
H	-1.974819	-2.436255	9.243680
C	-0.441509	-1.117765	8.623247
C	0.000552	0.055037	7.708453
C	-0.883075	0.196026	6.326054
H	-5.523504	-2.617114	6.049262
H	-5.762681	-1.930561	3.658352
H	-4.109853	-2.777273	8.096991
C	-0.725345	-0.090413	1.264237
C	-2.132487	-0.342951	1.252673
C	2.187884	-0.227947	6.203137
C	1.589452	0.153381	7.552928
C	-0.780626	0.089644	-1.203138
C	-2.143765	-0.122004	-1.197300
H	-2.698525	-0.122490	-2.143220
C	-2.856612	-0.375815	0.006828
C	-4.239879	-0.718248	0.043492
C	-4.869021	-1.067321	1.217313
C	4.403190	-0.450879	7.378541

C	3.748626	-0.599572	8.593699
H	4.323446	-0.872159	9.491020
C	2.351125	-0.503899	8.705492
C	0.332159	-1.324502	9.829132
C	1.676686	-1.029954	9.835238
H	5.493499	-0.533927	7.307129
H	2.285686	-1.307980	10.707791
H	-0.127177	-1.849993	10.675007
H	-5.922356	-1.367567	1.206968
H	-4.799583	-0.731106	-0.899339
H	-0.253243	0.253860	-2.149120
O	0.221378	1.766826	4.812915
O	-1.795529	1.186964	6.458500
O	1.873078	1.603779	7.658614
H	2.816951	1.647956	7.445488
O	-0.390425	1.186779	8.511616
<u>H</u>	<u>0.057535</u>	<u>1.025910</u>	<u>9.356766</u>

Table S15. Cartesian coordinates (Å) of geometry structure of product for the reaction of O₂@GO(14R)-1 and H₂O via a 4e-pathway at the B3LYP/def2-SVP level.

C	-0.045085	0.048412	2.534247
C	1.389122	0.157739	2.530144
C	2.074815	0.299933	1.291525
C	1.354907	0.379029	0.078134
C	-0.737840	-0.090492	3.764603
C	2.111806	-0.017316	3.764097
C	1.425903	-0.088183	5.009906
C	-0.016186	0.432950	5.028155
C	3.602763	-0.539636	6.123756
C	4.261596	-0.385460	4.890876
C	3.544436	-0.120985	3.717117
C	4.216617	0.064516	2.452538
C	3.520282	0.290634	1.301376
H	4.048880	0.429485	0.352575
H	5.311299	0.019970	2.435551
H	1.899658	0.524405	-0.860400
H	5.351815	-0.486777	4.847488
C	-4.107115	-1.258051	2.490668
C	-4.676613	-1.731730	3.685105
C	-3.971613	-1.684244	4.911495
C	-2.674399	-1.057809	4.978439
C	-2.049084	-0.591969	3.748700

C	-2.759787	-0.739576	2.505589
C	-4.509492	-2.245007	6.110558
C	-1.992362	-0.928202	6.207249
C	-2.531510	-1.543774	7.363249
C	-3.791301	-2.199900	7.287107
C	-1.793558	-1.522086	8.599952
H	-2.224307	-2.063786	9.453077
C	-0.565864	-0.945310	8.743563
C	0.063951	-0.053215	7.667262
C	-0.882943	0.123628	6.350879
H	-5.491322	-2.727540	6.076485
H	-5.680758	-2.166978	3.665614
H	-4.194785	-2.664590	8.193909
C	-0.736473	-0.039161	1.288149
C	-2.122750	-0.391203	1.276725
C	2.159645	-0.366685	6.194321
C	1.513924	-0.473366	7.462856
C	-0.799413	0.160337	-1.172655
C	-2.142212	-0.148833	-1.171848
H	-2.694690	-0.182468	-2.117377
C	-2.836418	-0.464725	0.032063
C	-4.191541	-0.899508	0.058768

C	-4.799302	-1.292588	1.232050
C	4.324609	-0.846407	7.317460
C	3.668108	-0.995679	8.515076
H	4.227112	-1.253331	9.421128
C	2.253649	-0.819910	8.608671
C	0.225168	-1.157541	9.937198
C	1.580995	-1.055978	9.878933
H	5.411059	-0.971587	7.257609
H	2.197844	-1.261209	10.760527
H	-0.270079	-1.489646	10.858177
H	-5.830938	-1.658215	1.217356
H	-4.745648	-0.947237	-0.885118
H	-0.283752	0.367860	-2.115894
O	0.181851	1.768947	4.891565
O	-1.649960	1.237723	6.650450
O	0.101647	1.267645	8.186637
H	<u>-0.750437</u>	<u>1.593664</u>	<u>7.578261</u>

Reference:

1. (a) Stankovich, S.; Dikin, D. A.; Piner, R. D.; Kohlhaas, K. A.; Kleinhammes, A.; Jia, Y.; Wu, Y.; Nguyen, S. T.; Ruoff, R. S., Synthesis of graphene-based nanosheets via chemical reduction of exfoliated graphite oxide. *Carbon* 2007, 45 (7), 1558-1565;
(b) Bhalerao, G. M.; Sinha, A. K.; Sathe, V., Defect-dependent annealing behavior of

- multi-walled carbon nanotubes. *Physica E: Low-dimensional Systems and Nanostructures* 2008, 41 (1), 54-59.
2. Ganguly, A.; Sharma, S.; Papakonstantinou, P.; Hamilton, J., Probing the Thermal Deoxygenation of Graphene Oxide Using High-Resolution In Situ X-ray-Based Spectroscopies. *J. Phys. Chem. C* 2011, 115 (34), 17009-17019.
3. Yamamoto, K.; Imaoka, T.; Chun, W. J.; Enoki, O.; Katoh, H.; Takenaga, M.; Sonoi, A., Size-specific catalytic activity of platinum clusters enhances oxygen reduction reactions. *Nat Chem* 2009, 1 (5), 397-402.
4. A. Ganguly, S. Sharma, P. Papakonstantinou and J. Hamilton, *J. Phys. Chem. C*, 2011, 115, 17009.
5. Z. Xu, Y. Bando, L. Liu, W. Wang, X. Bai and D. Golberg, *ACS Nano*, 2011, 5, 4401.
6. (a) Coutanceau, C.; Croissant, M. J.; Napporn, T.; Lamy, C., Electrocatalytic reduction of dioxygen at platinum particles dispersed in a polyaniline film. *Electrochim. Acta* 2000, 46 (4), 579-588; (b) Wu, G.; More, K. L.; Johnston, C. M.; Zelenay, P., High-Performance Electrocatalysts for Oxygen Reduction Derived from Polyaniline, Iron, and Cobalt. *Science* 2011, 332 (6028), 443-447.
7. Sidik, R. A.; Anderson, A. B.; Subramanian, N. P.; Kumaraguru, S. P.; Popov, B. N., O₂ Reduction on Graphite and Nitrogen-Doped Graphite: Experiment and Theory. *J. Phys. Chem. B* 2006, 110 (4), 1787-1793.
8. M. J. Frisch et al. Gaussian09 (Revision A. 02) (Gaussian, W. C., 2009).
9. F.Neese, O., 2.6; University of Bonn: Germany, 2008.

10. Neese, F.; Wennmohs, F.; Hansen, A.; Becker, U., Efficient, approximate and parallel Hartree–Fock and hybrid DFT calculations. A ‘chain-of-spheres’ algorithm for the Hartree–Fock exchange. *Chem. Phys.* 2009, 356 (1–3), 98-109.
11. Weigend, F.; Ahlrichs, R., Balanced basis sets of split valence, triple zeta valence and quadruple zeta valence quality for H to Rn: Design and assessment of accuracy. *Phys. Chem. Chem. Phys.* 2005, 7 (18), 3297-3305.
12. Zheng, Y.; Jiao, Y.; Chen, J.; Liu, J.; Liang, J.; Du, A.; Zhang, W.; Zhu, Z.; Smith, S. C.; Jaroniec, M.; Lu, G. Q.; Qiao, S. Z., Nanoporous Graphitic-C₃N₄@Carbon Metal-Free Electrocatalysts for Highly Efficient Oxygen Reduction. *J. Am. Chem. Soc.* 2011, 133 (50), 20116-20119.